Journal of Hepatocellular Carcinoma

Dovepress
Taylor & Francis Group

Open Access Full Text Article

ORIGINAL RESEARCH

Cms1 Ribosomal Small Subunit Homolog Promotes HCC Proliferation and Migration by Modulating the TNF/NF-κB Signaling Pathway

Tuo Zhang[1,*], Yongping Huang[2,*], Sha Hu[2], Yongjie Yu[2], Fang Qin[2], Yu Zhang[2], Zeming Cai[3], Haitao Wang[2], Peng Zhang[2], Jing Dai[1,4]

[1]Department of Radiation and Medical Oncology, Zhongnan Hospital of Wuhan University, Wuhan, Hubei, 430071, People's Republic of China; [2]Wuhan University Taikang Medical School (School of Basic Medical Sciences), Wuhan, Hubei, 430071, People's Republic of China; [3]Department of Cardiology, Renmin Hospital of Wuhan University, Wuhan, Hubei, 430060, People's Republic of China; [4]Hubei Key Laboratory of Tumor Biological Behaviors, Zhongnan Hospital of Wuhan University, Wuhan, Hubei, 430071, People's Republic of China

*These authors contributed equally to this work

Correspondence: Jing Dai, Department of Radiation and Medical Oncology, Zhongnan Hospital of Wuhan University, 169 East Lake Road, Wuchang District, Wuhan, Hubei, 430071, People's Republic of China, Email daijing@znhospital.cn; Peng Zhang, Wuhan University Taikang Medical School (School of Basic Medical Sciences), 115 East Lake Road, Wuchang District, Wuhan, Hubei, 430071, People's Republic of China, Email zhp@whu.edu.cn

Purpose: The study aims to further classify hepatocellular carcinoma (HCC) based on proliferative capacity, identify hub genes associated with highly proliferative HCC, and investigate its regulatory roles in HCC.

Materials and Methods: Bioinformatics analysis was employed to establish classification of HCC and further identify the hub gene. Cell counting kit-8 (CCK-8) assay, colony formation assay, Western Blot assay and tumor xenograft assay were employed to detect the proliferation of HCC cells. Transwell assay and Western blot assay were employed to detect the migration of HCC cells. RNA sequencing analysis was employed to explore the signaling pathways activated by the gene and verify it through rescue experiments.

Results: We classified HCC into three more precise subtypes termed Prolifer-low, Prolifer-mid and Prolifer-high, and also found that Cms1 ribosomal small subunit homolog 1 (CMSS1) was a hub gene associated with stronger proliferative capacity subgroup of HCC. Functional studies revealed that CMSS1 overexpression significantly promoted the proliferation of HCC cells in vitro and in vivo. Additionally, CMSS1 could also promote the migration and epithelial-mesenchymal transition of HCC cells. Mechanistically, RNA sequencing analysis revealed that CMSS1 knockdown inhibited the tumor necrosis factor (TNF) and downstream nuclear factor kappa B (NF-κB) signaling pathways. More importantly, TNF or NF-κB suppression could reverse the promoting effects of CMSS1 on HCC cells proliferation and migration.

Conclusion: The study suggested that CMSS1 could be a critical modulator of HCC tumorigenesis and metastasis through the TNF/NF-κB signaling pathway, thus being considered as a potential therapeutic target for HCC. Targeting CMSS1 may offer a novel strategy to inhibit NF-κB-driven inflammatory signaling and suppress tumor progression in HCC.

Keywords: CMSS1, HCC, proliferation, migration, TNF, NF-κB

Introduction

According to the Global Cancer Statistics 2022, liver cancer is the sixth most common type of cancer, with the third highest mortality rate.[1] Hepatocellular carcinoma (HCC) accounts for ~80% of all primary liver cancers.[2] The burden of HCC varies significantly across different regions, and China is the nation bearing the greatest burden of HCC, globally.[3] Currently, the surgical treatment approach still offers the best long-term survival prospects for patients with HCC.[4] However, a significant proportion of patients with HCC are diagnosed in advanced stages of the disease and can be therefore treated only with systemic therapies.[5] With the development of medical technology, systemic therapy has transitioned from single-agent targeted therapy to

Received: 23 June 2025
Accepted: 10 October 2025
Published: 28 October 2025

combination therapy, thus resulting in significant stride. Unfortunately, the clinical treatment of HCC is very challenging, since only a small proportion of patients can achieve positive clinical benefits.[6]

Classification can assist in a deeper understanding of diseases. HCC can be also stratified into two major classes based on its molecular subtype, the proliferation class and the non-proliferation class.[7] The non-proliferation subtype maintains the expression of hepatocyte differentiation-related markers and displays chromosomal stability, thus being associated with a well-differentiated phenotype.[8,9] In addition, the proliferation subtype is more common in patients with hepatitis B infection. This HCC subtype is commonly characterized by the presence of TP53 mutations, chromosomal instability, upregulation of cell cycle-related genes, and activation of classical cell proliferation-related pathways, such as the RAS/mitogen-activated protein kinase (MAPK) and phosphatidylinositol 3-kinase/protein kinase B signaling pathways.[8,9] Furthermore, patients with this HCC subtype commonly present with elevated serum alpha-fetoprotein levels and poor clinical prognosis.[10] Therefore, understanding the molecular mechanisms underlying the development of proliferative HCC and identify new therapeutic targets are of significant importance.

Herein, to uncover the mechanism of proliferative HCC, bioinformatics analysis was performed to establish a more precise classification of HCC based on its proliferative capacity and identify hub genes associated with the high-proliferative capacity subgroup. Furthermore, the most significant hub gene, namely Cms1 ribosomal small subunit homolog 1 (CMSS1), was further explored regarding its role in cell proliferation. CMSS1 was a relatively understudied molecule currently recognized as an RNA binding protein (RBP).[11] The latest research indicated that CMSS1 played a significant role in the progression and prognosis of non-small cell lung cancer.[12,13] In the study, we provided novel insights into the mechanism of CMSS1 in HCC progression.

Materials and Methods

Data Collection

The gene expression profile and clinical data from a total of 369 HCC samples and 50 adjacent control tissue samples were obtained from The Cancer Genome Atlas (TCGA; https://portal.gdc.cancer.gov/). The RNA-seq data for the GSE138485, GSE214846, GSE124535 and GSE151530 datasets were collected from the Gene Expression Omnibus database (https://www.ncbi.nlm.nih.gov/geo/). The involved human data were approved by the Medical Ethics Committee, Zhongnan Hospital of Wuhan University.

Consensus Clustering Analysis

Consensus clustering analysis was performed using the "ConsensusClusterPlus" in R package, following the standard procedure outlined in the instructions. Subgroups were divided based on the 697 proliferation-related gene sets in the Hallmark term (Table S1), with a resampling frequency of 1,000 (reps=1,000) and default parameters for the rest. The optimal number of clusters was determined according to the following three criteria: i. The area under the consensus cumulative distribution function (CDF) curve should tend to stabilize; ii. the number of samples allocated to each cluster should be appropriate and stable; and iii. the clustering heatmap should be clear and not mixed. After comprehensive consideration, a K value of three was considered to indicate the optimal number of clusters in the current clustering analysis.

Bulk RNA-Seq-Related Data Analysis

The offline RNA-seq data was subjected to FastQC (v0.12.1) data quality control and were then aligned with the human reference genome (hg38) using HISAT2 (v2.2.1). Raw counts and transcripts per million (TPM) were quantitatively obtained by StringTie (v2.2.3). Principal component and differential gene analyses were carried out using "gmodels" and "DESeq2" in R package. The screening criteria for differentially expressed genes are explained in the results section of the manuscript. Herein, single sample gene set enrichment analysis (ssGSEA) was performed using "GSVA" in R package, while GSEA was conducted using "clusterProifler". Kyoto Encyclopedia of Genes and Genomes (KEGG) enrichment analysis of the differentially expressed genes was directly carried out to reveal the statistical significance of each pathway using hypergeometric distribution based on the gene pathway annotation file provided on the official website.

Clinical Prognostic Analysis

The overall survival time and disease-free interval were obtained from TCGA official website. Kaplan Meier estimation and curve drawing were performed using "survival" and "survivminer" in R package.

Single Cell RNA-Seq Data Analysis

The single cell RNA-seq data from HCC samples was included in the GSE151530 dataset. Data were processed using "Seurat" (v5.0) in R package. Low quality cells were filtered using the following criteria: 500<nFeature-RNA<8,000 genes and mitochondrial gene content of <20%. A total of 40,270 high-quality cells were eliminated from the batch effects using "Harmony", and then dimensionality was reduced using UMAP. The "Louvain" algorithm was used to partition cell clusters with a resolution of 0.2. Finally, the cell types were identified based on publicly available cell markers.

Cell Lines and Cell Culture

293T cells and the human HCC cell lines, HepG2, MHCC97H, Huh7, MHCC97L, HLF and PLC/PRF/5, were obtained from the American Type Culture Collection. In addition, the above HCC cell lines were authenticated using short tandem repeat (STR) profiles. All cells were cultured in DMEM (Procell Life Science & Technology Co., Ltd)., containing 10% fetal bovine serum (FBS; NEWZERUM, Ltd.) and 1% penicillin/streptomycin solution (Procell Life Science & Technology Co., Ltd.) at 37°C with 5% CO_2.

Western Blot Analysis

For Western blot analysis, total protein extracts were isolated from tissue or cell samples using SDS lysis buffer (Sinopharm Chemical Reagent Co., Ltd.) followed by quantification. An equal amount of protein extracts was separated by 10% SDS-PAGE, followed by transferring onto PVDF membranes (Millipore; Sigma). Following sealing in 5% skim milk for 1 h, the membrane was incubated overnight with a primary antibody at 4°C and then with the corresponding secondary antibodies at room temperature for 1 h. The antibodies used in the current study are listed in Table S2.

Reverse Transcription-Quantitative PCR (RT-qPCR) Assay

For RT-qPCR assays, total RNA was extracted from tissue or cell samples using a Trizol reagent (Sigma-Aldrich; Merck KGaA). Subsequently, the isolated total RNA was reversed transcribed into cDNA using the HiScript III RT SuperMix for qPCR (+gDNA wiper) kit (Vazyme Biotech Co., Ltd). The ChamQ SYBR qPCR Master Mix kit (Vazyme Biotech Co., Ltd.) was used to detect the PCR amplification products. The mRNA expression levels were calculated as fold change using the standard formula. The primer sequences used are listed in Table S3.

Establishment of a Stable CMSS1 Overexpressing Cell Line

293T cells were seeded into 6-well plates (Wuxi NEST Biotechnology Co., Ltd.) at a density of 6×10^5 cells/well until they reached 70% confluence on the second day. Subsequently, the targeted plasmids, pSPAX2 and pMD2.G were co-transfected into 293T cells for 48 h and the supernatant containing sufficient lentivirus was then collected and used to infect Huh7 and HepG2 cells in 6-well plates. Following incubation for 48 h, wild-type cells served as the control group, while the stable CMSS1 overexpressing cells were screened with 2 μg/mL puromycin dihydrochloride (Beyotime Institute of Biotechnology). The culture medium was then replaced and the stable expressing cells were selected. The successful establishment of the stable cell line was verified using Western blot and RT-qPCR analyses. The primer sequences used are listed in Table S3.

Cell Counting Kit-8 (CCK-8) Assay

The stable CMSS1 overexpressing cells were seeded in 96-well plates (Wuxi NEST Biotechnology Co., Ltd.) at a density of 3×10^3 cells/well in 100 μL culture medium (n=5 replicates). The culture medium was then replaced with fresh one, supplemented with 10% CCK-8 reagent (Beyotime Institute of Biotechnology) and cells were then cultured for 0, 24, 48, 72 and 96 h. Following incubation at 37°C for 120 min, the absorbance values in each well were measured at a wavelength of 450 nm using an enzyme labeler (Thermo Fisher Scientific, Inc).

Colony Formation Assay

Cells were seeded into 6-well plates (Wuxi NEST Biotechnology Co., Ltd.) and cultured for 14 days, with the intermediate being changed every three days to maintain the growth environment of the cells. When reached the indicating planned time, colonies were washed with PBS and were then fixed with 4% paraformaldehyde (Wuhan Servicebio Technology Co., Ltd.) for 15 min. After fixing, the formed colonies were stained with crystal violet staining solution (Beyotime Institute of Biotechnology) for 20 min. Finally, the cells were washed again with PBS to remove any excess dye and images of the culture plates were captured under a digital single lens reflex camera.

Transwell Migration Assays

The Transwell chambers (Corning, Inc.) were placed on 24-well plates (NEST) and cells in 100 μL culture medium without FBS were seeded into the upper chamber at a density of 8×10^4 cells/well. The lower chamber was supplemented with 600 μL DMEM containing 10% FBS. Following incubation for two days, the non-migrated cells were cautiously removed from the upper chamber, while the migrated ones in the lower chamber were fixed with 4% formaldehyde and were then stained with crystal violet staining solution for 10 min.

Xenograft Mouse Model

To establish a xenograft mouse model, HepG2 cells (density, 5×10^6 cells per mouse) transfected with CMSS1 overexpressing plasmid or control vector were separately suspended in 200 μL PBS and were then injected into the backs of 4-week-old male nude mice. As the tumor began to grow, the weight of the mice was measured every two days. The tumor volume was also recorded. On the last day of the experiment, the mice were euthanized by cervical dislocation following anesthesia by intraperitoneal injection of 0.3% sodium pentobarbital (30 mg/kg). Euthanasia was confirmed by verifying respiratory and cardiac arrest, along with pupil dilation, for a minimum of 10 min. Then, images of the naked mice were captured, and the size and weight of the tissue samples were measured. The maximum tumor diameter and volume were <1 cm and <1,000 mm^3, respectively. All animal experimental protocols were approved by the Animal Care and Use Committee of the Renmin Hospital of Wuhan University and performed in accordance with the "Laboratory animal—Guideline for welfare and ethics" (GB/T 35892–2018) issued by the Standardization Administration of China.

Immunohistochemistry (IHC) Assay

IHC analyses were performed using paraffin-embedded tissue sections, which were subjected to dewaxing. Antigen retrieval was carried out in heat-induced sodium citrate buffer (pH, 6.0). Subsequently, the tissue sections were incubated with the primary antibody at 4°C overnight and then with the corresponding secondary antibody (Wuhan Servicebio Technology Co., Ltd.) at 37°C for 1 h. The immunoreactive signal was developed using 3,3′-diaminobenzidine (DAB) solution (ZSGB-BIO). The sources and dilutions of the primary antibodies used are listed in Table S2.

Statistical Analysis

Statistical analysis was performed using SPSS version 25 software (IBM Corp.) and graphs were constructed using GraphPad Prism 8.0 (GraphPad Software, Inc). The statistically significant differences in TPM differential expression or clinical indicators between normal and tumor samples were evaluated by Wilcoxon rank-sum test. The Student's *t*-test or analysis of variance (ANOVA) was used to analyze the statistical significance between different groups. The data are expressed as the mean ± SD. $P<0.05$ was considered to indicate a statistically significant difference (*P< 0.05; **P<0.01; ***P<0.001; ns, not significant).

Results

HCC Subtypes with Strong Proliferative Ability Have Poor Prognosis

The proliferation ability of liver tumor cells varies among different patients with HCC. Therefore, based on the differences in the proliferation rate, patients with HCC can be divided into different subgroups. Herein, a total of 696 genes associated with proliferation was screened using the Hallmark gene set in MSigDB (Table S1). Based on the

expression of these genes, 369 patients with HCC in TCGA were classified into different subgroups with different proliferative abilities through consensus clustering (Figure 1A). Subsequently, through consensus CDF and consistency of sample clustering, three clusters were determined as the optimal number of clusters (Figure 1B and Figure S1A–S1C).

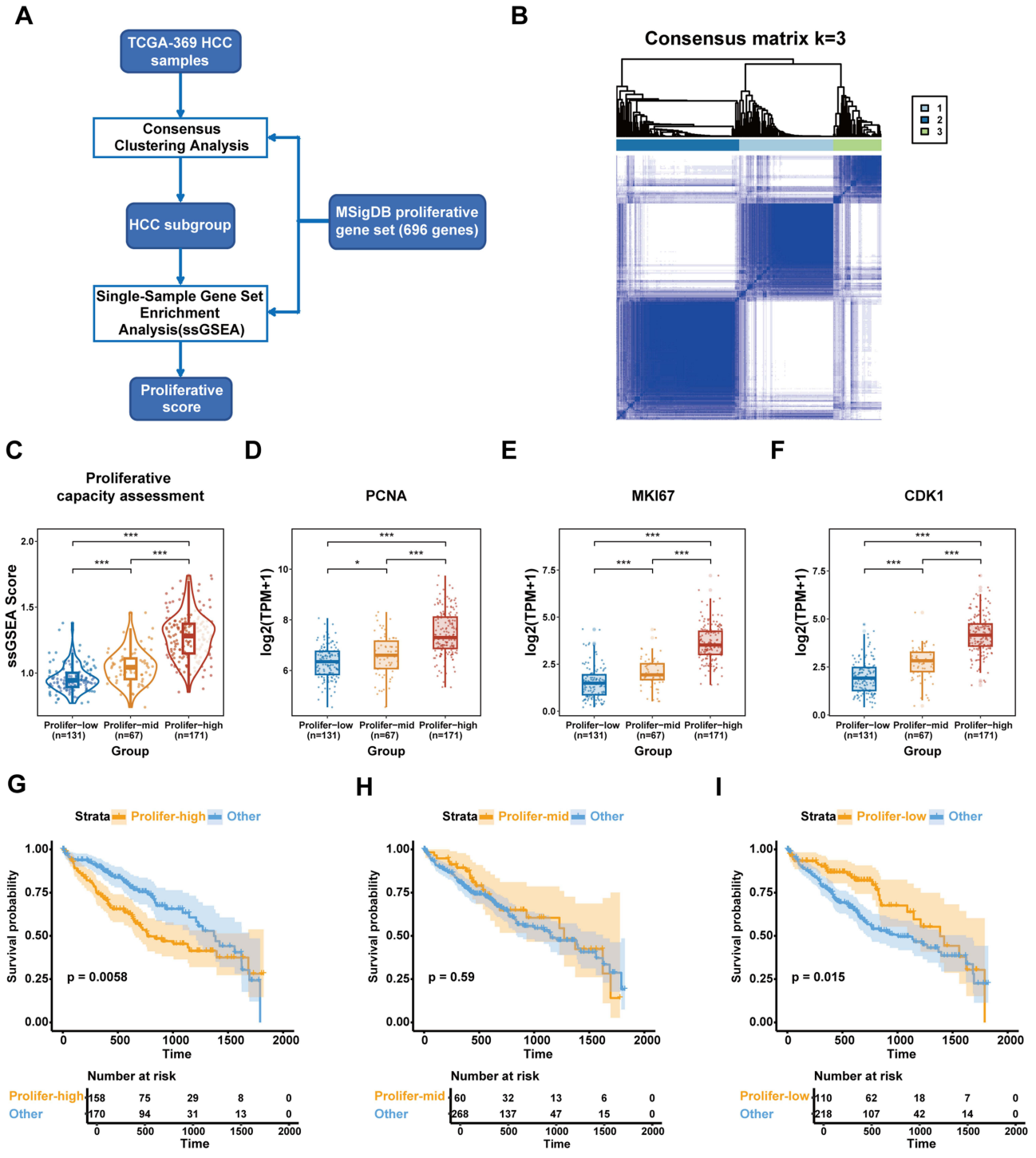

Figure 1 HCC subtypes with strong proliferative ability have poor prognosis. (**A**) Schematic illustration of the analytical approach. (**B**) Heatmap of Consensus Clustering Analysis (k=3). (**C**) The proliferation score, calculated by ssGSEA and (**D**–**F**) the expression levels of proliferation markers PCNA, MKI67, CDK1 for three subgroups (Prolifer-low, n=131; Prolifer-mid, n=67; Prolifer-high, n=171). (**G**–**I**) The Kaplan-Meier curve shows that the Prolifer-high subgroup has a lower 5-year survival rate, while the Prolifer-low subgroup has a higher 5-year survival rate. All data are presented as the means ± SD, *p < 0.05; **p < 0.01; ***p < 0.001.

Abbreviations: ns, not significant; ssGSEA, single sample gene set enrichment analysis; PCNA, proliferating cell nuclear antigen; MKI67, marker of proliferation Ki-67; CDK1, cyclin dependent kinase 1.

https://doi.org/10.2147/JHC.S549003

In addition, the proliferation capacity in the above three subgroups was evaluated using ssGSEA. According to their ssGSEA scores and the expression of the aforementioned proliferation-related genes, cells were allocated into the Prolifer-low, Prolifer-mid and Prolifer-high subpopulations (Figure 1C). Furthermore, the expression levels of the proliferation-related markers, proliferating cell nuclear antigen (PCNA), marker of proliferation Ki-67 (MKI67) and cyclin-dependent kinase 1, were consistent with the grouping (Figure 1D–F). The above results indicated that patients with HCC could be categorized into three subgroups with low, medium and high proliferative capacity.

To reveal the functional characteristics of each subgroup, the gene sets of Reactome, KEGG and wikipathway were derived from MSigDB. Then, the enriched biological processes in each subgroup were identified through GSEA. Therefore, genes in the Prolifer-high subgroup were mainly associated with proliferation, and more particularly with "DNA strand elongation" and "DNA replication" (Figure S1D). In addition, genes in the Prolifer-mid subgroup were primarily enriched in terms associated with mitochondrial assembly and protein trafficking, such as "complex III assembly" and "protein export" (Figure S1E). Finally, the key events in the Prolifer-low subgroup were mainly involved in lipid metabolism and redox-related processes, including "fatty acid metabolism" and "oxidation by cytochrome P450" (Figure S1F). Subsequently, the prognosis in the above three subgroups was evaluated. Therefore, the Profiler-high subgroup was significantly associated with poor prognosis, the Prolifer-low subgroup with good prognosis, while no significant association was obtained between the Prolifer-mid subgroup and prognosis (Figure 1G–I). The aforementioned results suggested that patients in the high proliferation subgroup could display poorer clinical treatment outcomes, and therefore more targeted treatment approaches should be developed for these patients.

CMSS1 Is a Potential Target in HCC Patients in the Prolifer-High Subgroup

According to the preceding results, the current study aimed to identify therapeutic targets particularly for patients in the Prolifer-high subgroup. Firstly, the association between each gene and the Prolifer-high subgroup was determined in TCGA liver tumor samples. Therefore, a total of 2,399 genes displayed a correlation value of >0.9 (Figure S2A). Subsequently, a total of 3,246 differentially expressed genes were identified to be upregulated in liver tumor samples compared with normal adjacent tissue samples. The screening criteria for the differentially expressed genes were as follows: Fold change (FC) >1.5 and adjust, pvalue <0.05 (Figure S2B). Finally, utilizing the publicly available GSE151530 single-cell dataset for HCC and following standard single-cell sequencing data analysis and marker identification, a total of 360 marker genes, that could be highly expressed in liver cells or liver tumor cells, were screened. The criteria for selecting these marker genes were the following: $\log_2$FC >0.25, pct1 >0.25 and pct2 <0.1 (Figure S2C–E). Through the above rigorous analysis, 24 target genes were identified to be strongly associated with the Profiler-high subgroup. The above target genes were particularly expressed in the liver, while they were involved in tumor progression (Figure 2A). Furthermore, the association between these target genes and HCC prognosis was evaluated through overall survival time and disease-free interval time. The results showed that *CMSS1, NECAB3, CDKN2A* and *TMEM106C* were risk factors for HCC (Figure 2B and C), with *CMSS1* being less studied compared with the remaining three genes. Therefore, *CMSS1* was selected as the target gene for further research. Subsequently, the association between CMSS1 expression and HCC progression was further investigated. As previously described, CMSS1 was significantly upregulated in TCGA HCC samples compared with adjacent normal tissue samples (Figure 2D). Consistent results were obtained in multiple paired public HCC datasets (Figure 2E–G). In addition, CMSS1 expression was significantly positively associated with HCC stage and grade (Figure 2H and I). In terms of fibrosis, CMSS1 was significantly upregulated in fibrotic samples compared with non-fibrotic ones, while its expression was declined in cirrhotic liver samples (Figure 2J). Finally, the Kaplan-Meier curve more clearly demonstrated the significant association between CMSS1 expression and poor prognosis (Figure 2K and L). In summary, the above results indicated that CMSS1 was highly associated with the occurrence and development of HCC.

CMSS1 Affects the Proliferation of HCC Cells

To uncover the biological functions of CMSS1 in HCC, the expression levels of CMSS1 were detected in different HCC cell lines. The results showed that the expression levels of CMSS1 were comparable among these cell lines (Figure S3A). Therefore, the two most commonly used HCC cell lines, namely HepG2 and Huh7, were employed to construct stable

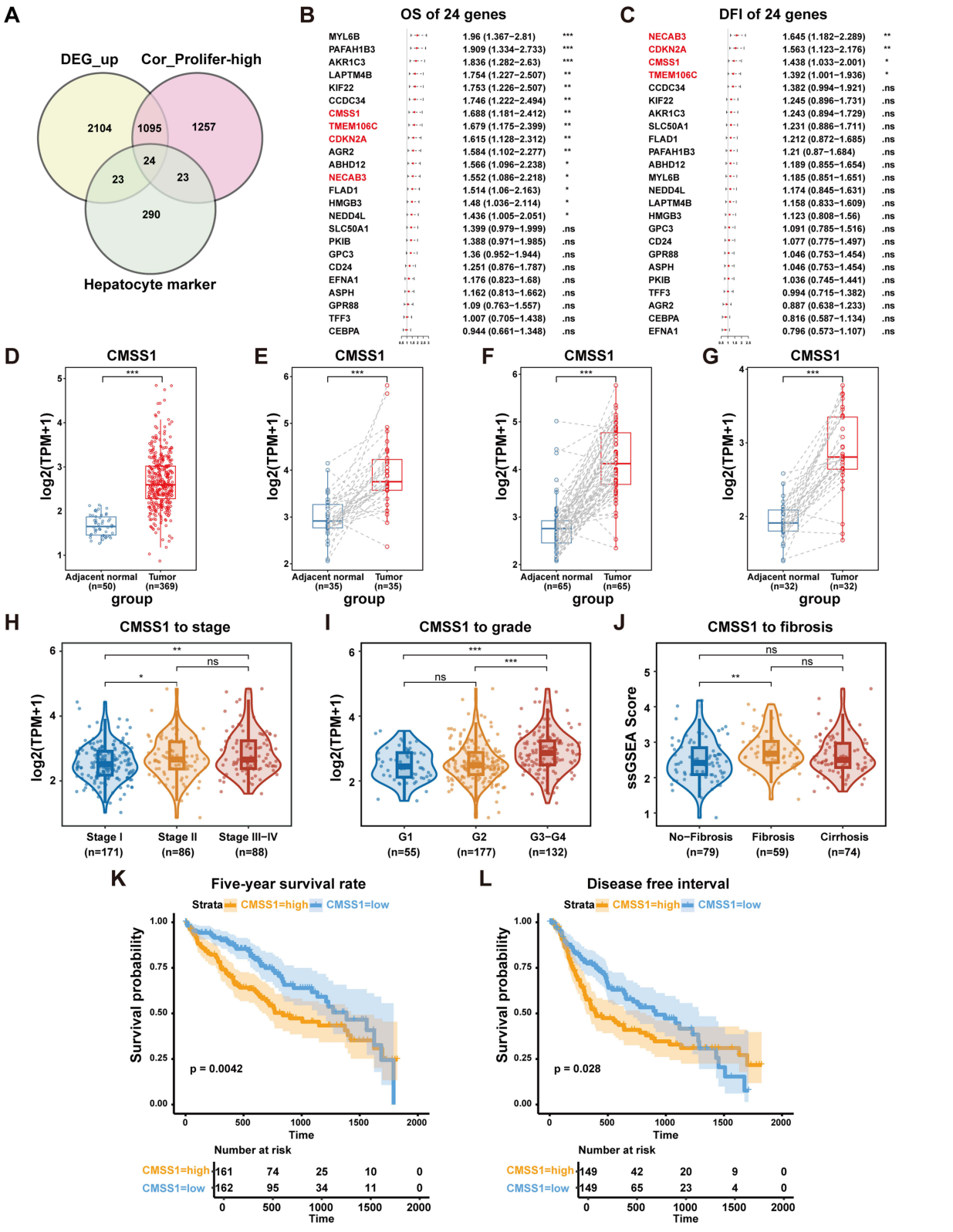

Figure 2 CMSS1 is a potential target for prolifer-high subgroup patients. (**A**) Screening for target genes that are highly correlated with the Prolifer-high subgroup, are highly expressed in tumors, and specifically expressed in hepatocytes or liver tumor cells. (**B** and **C**) Prognosis of overall survival time and disease-free interval time of 24 genes. (**D**) The expression of CMSS1 in TCGA HCC samples is upregulated compared to adjacent normal samples. (**E**–**G**) In multiple paired public HCC datasets, CMSS1 expression was upregulated in HCC samples compared to adjacent normal samples. (**H** and **I**) The expression of CMSS1 is positively correlated with the stage and grade of HCC. (**J**) CMSS1 expression significantly increased only in fibrosis samples. (**K** and **L**) The Kaplan-Meier curve show that tumor patients with high expression of CMSS1 have a lower 5-year survival rate and disease-free interval. All data are presented as the means ± SD, *p < 0.05; **p < 0.01; ***p < 0.001.

https://doi.org/10.2147/JHC.S549003

CMSS1-overexpressing and CMSS1-depleted cell lines (Figure S3B–F). The CCK-8 assay showed that the CMSS1 overexpression group of HepG2 cells had higher OD values, and the cell colony formation assay indicated that the CMSS1 overexpression group had more colonies, while the CMSS1 knockdown group exhibited the opposite effect (Figure 3A–C). In addition, the Western blot results demonstrated that CMSS1 overexpression upregulated PCNA and cyclin D1 in HepG2 cells (Figure 3D). The opposite effect was observed in CMSS1-depleted HepG2 cells (Figure 3E). Consistent results were obtained in the Huh7 cell line (Figure S4A–E). These results suggested that CMSS1 overexpression could promote the proliferation of HCC cells in vitro.

To further verify the effect of CMSS1 on tumor formation in vivo, HepG2 cells stably transfected with CMSS1 overexpression plasmid or control vector were subcutaneously injected into the right back of nude mice to establish a xenograft mouse model. Compared with the control group, tumor volume and weight were increased in the CMSS1 overexpression group (Figure 3F–H). Subsequently, the enhanced mRNA and protein expression levels of CMSS1 in the CMSS1 overexpression group compared with the control group were verified (Figure S4F and G). Furthermore, the xenograft tumor tissues were also subjected to hematoxylin and eosin (H&E) staining and IHC analysis (PCNA and MKI67; Figure 3I). And the IHC analysis showed that the CMSS1 overexpression group had a higher positive rate of PCNA and MKI67. The above findings verified that CMSS1 overexpression could promote the growth of HCC cells.

CMSS1 Affects the Migration and Epithelial-Mesenchymal Transition (EMT) of HCC Cells

It has been reported that poor prognosis in HCC is commonly associated with high metastatic ability.[14] Therefore, herein, the role of CMSS1 in regulating the metastatic ability of HCC cells was further explored. The results of Transwell migration assays showed that CMSS1 overexpression notably promoted the metastasis of HCC cells (Figure 4A and B). Conversely, CMSS1 knockdown remarkably inhibited the metastasis of HCC cells (Figure 4C and D). To further uncover the potential mechanisms underlying the effect of CMSS1 on regulating the metastatic abilities of HCC cells, the association between CMSS1 and EMT, a process intimately associated with tumor metastasis,[15,16] was assessed. The Western blot results showed that CMSS1 overexpression upregulated N-cadherin and downregulated E-cadherin, while CMSS1 knockdown had the opposite effect (Figure 4E–H). The aforementioned findings suggested that CMSS1 could regulate the metastatic ability of HCC cells via modulating EMT.

CMSS1 Activates the Tumor Necrosis Factor (TNF) Signaling Pathway

Subsequently, the current study aimed to elucidate the mechanisms underlying the effect of CMSS1 on modulating the progression of HCC. Therefore, transcriptomic sequencing was carried out on CMSS1-depleted and control Huh7 cells. CMSS1 expression was detected in the RNA sequencing results, thus indicating the successful knockdown of CMSS1 (Figure S5A). The principal component analysis showed significant intergroup differences and high intragroup consistency between the CMSS1 knockdown and control groups (Figure S5B). Subsequently, differential expression gene analysis revealed that 1,133 genes were downregulated following CMSS1 knockdown (Figure S5C). Furthermore, KEGG enrichment analysis was conducted on the above genes to identify the signaling pathways that could be inhibited after CMSS1 knockdown. The results showed that the TNF signaling pathway was most significantly inhibited (Figure 5A). In addition, the expression of major downstream genes was also significantly suppressed (Figure 5B). To verify whether CMSS1 could affect the TNF pathway, the expression levels of the TNF pathway downstream genes, *TNF, CSF1, CXCL2* and *CXCL5*, were detected. The RT-qPCR results demonstrated that CMSS1 knockdown reduced the expression levels of these genes, while CMSS1 overexpression displayed the opposite effect (Figure S5D and E). More importantly, cell treatment with the TNF pathway inhibitor, R-7050, diminished the activation of the TNF pathway and the CMSS1 overexpression-mediated tumor promoting effects of HpeG2 and Huh7 cells (Figure 5C–H). Overall, these results indicated that CMSS1 could promote HCC proliferation and migration via modulating the TNF signaling pathway.

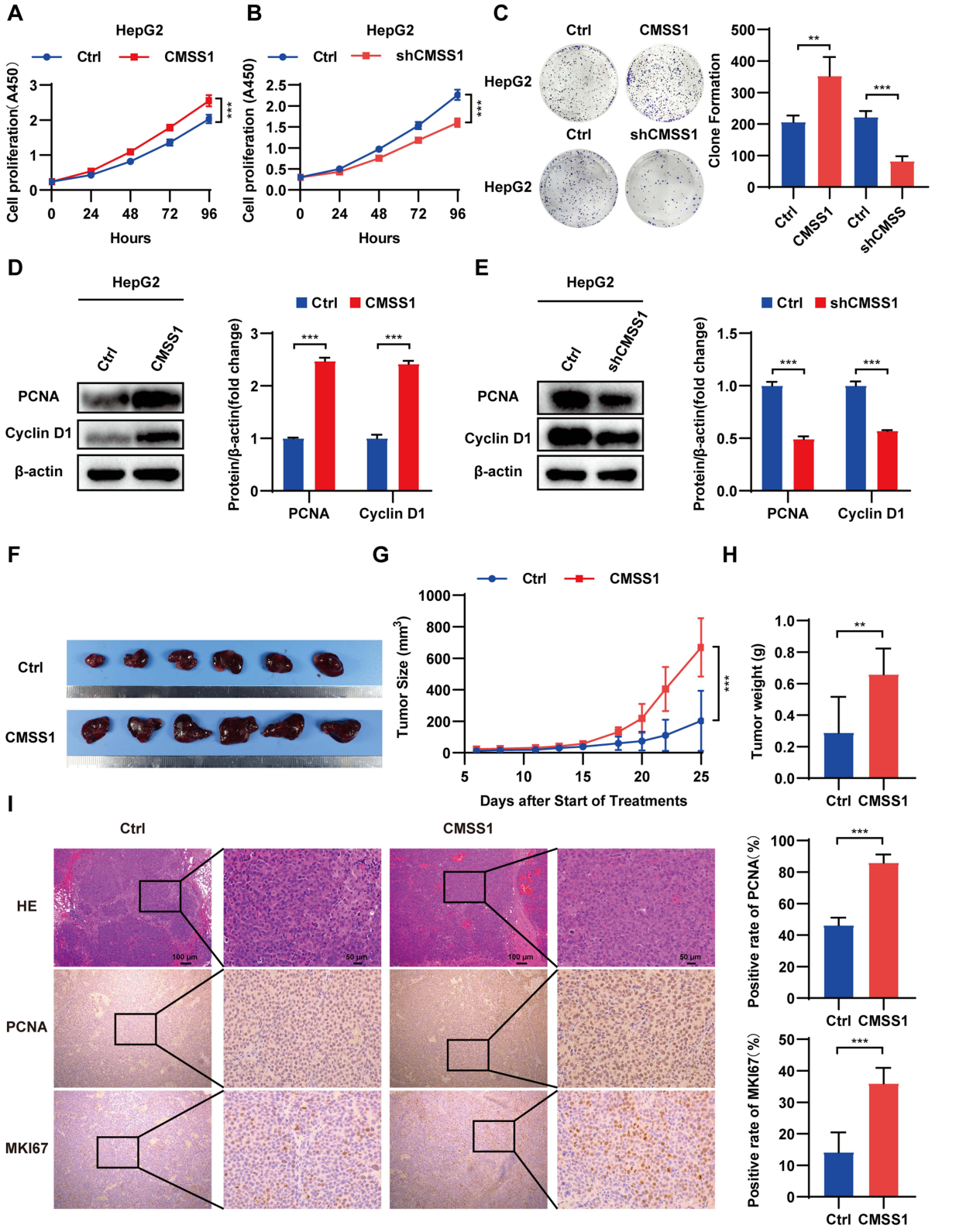

Figure 3 CMSS1 overexpression affects the proliferation of HCC cells. (**A** and **B**) CCK-8 assay showed that CMSS1 overexpression promoted proliferation capacity of HepG2 cells, whereas CMSS1 knockdown had the opposite effects. (**C**) Colony formation assay showed that CMSS1 overexpression promoted proliferation capacity of HepG2 cells, whereas CMSS1 knockdown had the opposite effects. (**D** and **E**) Western blot assay showed that CMSS1 overexpression promoted the proliferation-related protein (PCNA and Cyclin D1) expression of HepG2 cells, whereas CMSS1 knockdown had the opposite effects. (**F**) Photographs of xenograft tumors induced by subcutaneously inoculating HepG2-transfected cells into nude mice. (**G**) Growth curves of xenograft tumor volumes showed that CMSS1 overexpression promoted the growth of xenograft tumors in vivo. (**H**) Graphs of xenograft tumor weights showed that CMSS1 overexpression promoted the growth of xenograft tumors in vivo. (**I**) Representative H&E staining and PCNA, MKI67 immunostaining of xenograft tumors (Scale bar, 50 μm and 100 μm). All data are presented as the means ± SD, *p < 0.05; **p < 0.01; ***p < 0.001.

Abbreviations: ns, not significant; PCNA, proliferating cell nuclear antigen; MKI67, marker of proliferation Ki-67.

https://doi.org/10.2147/JHC.S549003

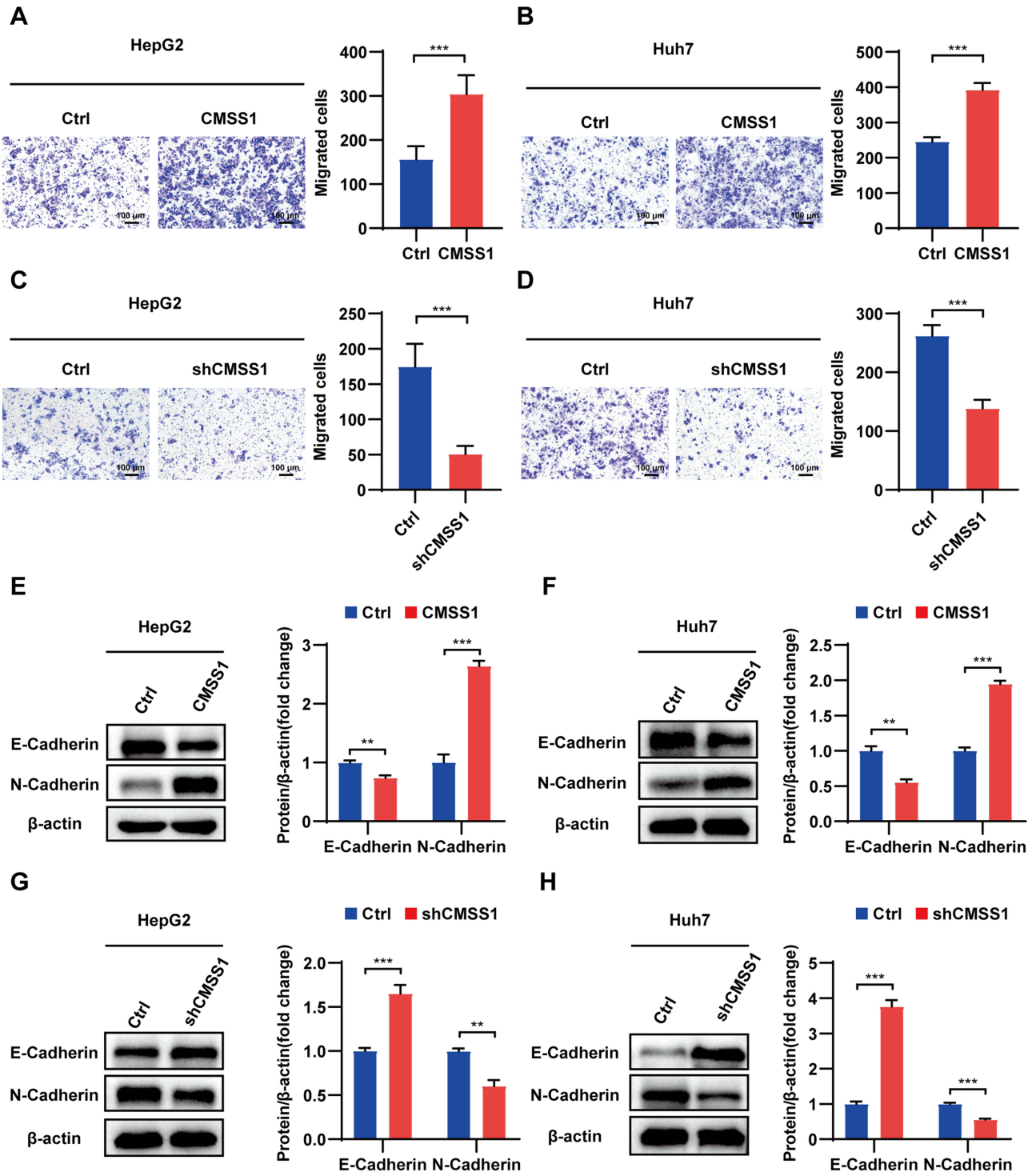

Figure 4 CMSS1 affects the migration and EMT of HCC Cells. (**A** and **B**) Transwell migration assay showed that CMSS1 overexpression promoted the migration capacity of HepG2 and Huh7 cells (Scale bar, 100 μm). (**C** and **D**) Transwell migration assay showed that CMSS1 knockdown inhibited the migration capacity of HepG2 and Huh7 cells (Scale bar, 100 μm). (**E** and **F**) Western blot assay showed the EMT-related protein (E-cadherin and N-cadherin) expression of HepG2 and Huh7 cells with control and CMSS1 overexpression groups. (**G** and **H**) Western blot assay showed the EMT-related protein (E-cadherin and N-cadherin) expression of HepG2 and Huh7 cells with control and CMSS1 knockdown groups. All data are presented as the means ± SD, *p < 0.05; **p < 0.01; ***p < 0.001.
Abbreviation: ns, not significant.

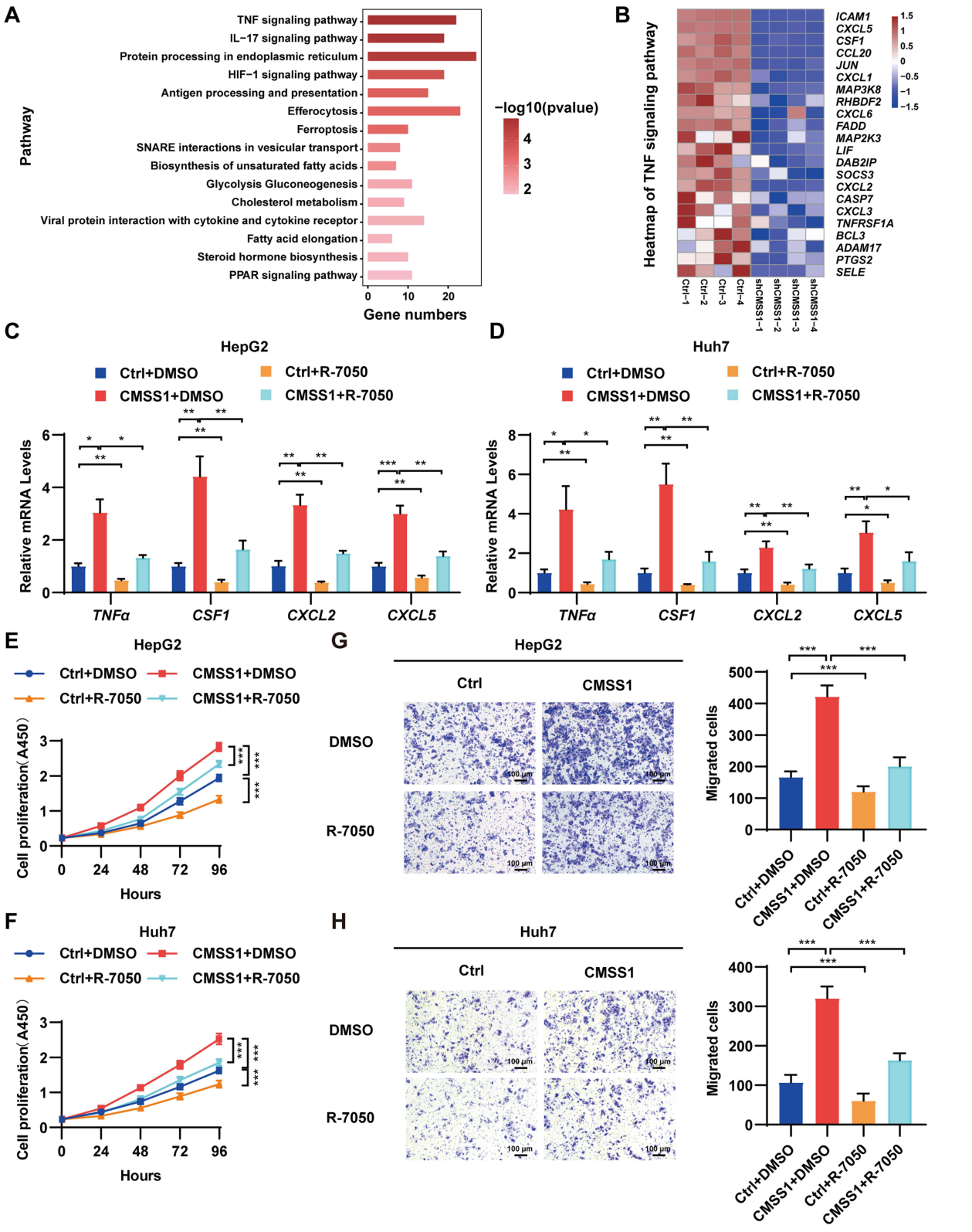

Figure 5 CMSS1 activates the TNF signaling pathway. (**A**) KEGG enrichment analysis reveals that TNF is the most significantly inhibited signaling pathway after CMSS1 knockdown. (**B**) The heatmap shows that the main downstream molecules of TNF are downregulated in expression after knocking down CMSS1. (**C** and **D**) RT-qPCR showed that R-7050 (1 μM) reversed the up-regulation of TNF pathway downstream genes expression levels caused by CMSS1 overexpression in HepG2 and Huh7 cells. (**E** and **F**) CCK-8 assay showed that R-7050 (1 μM) reversed the enhanced proliferation capacity caused by CMSS1 overexpression in HepG2 and Huh7 cells. (**G** and **H**) Transwell migration assay showed that R-7050 (1 μM) reversed the enhanced migration capacity caused by CMSS1 overexpression in HepG2 and Huh7 cells. All data are presented as the means ± SD, *p < 0.05; **p < 0.01; ***p < 0.001.
Abbreviations: ns, not significant; RT-qPCR, reverse transcription-quantitative PCR.

https://doi.org/10.2147/JHC.S549003

CMSS1 Promotes HCC Tumorigenesis via Activating the TNF/Nuclear Factor Kappa B (NF-κB) Signaling Pathway

Since the TNF signaling pathway is involved in regulating tumor growth via activating the NF-κB pathway in several types of malignant tumors,[17–19] the current study further investigated whether CMSS1 could also promote tumor cell proliferation and metastasis via activating NF-κB signaling. The results showed that CMSS1 overexpression and silencing could activate and inhibit the NF-κB pathway, respectively (Figure 6A and B). In addition, HpeG2 and Huh7 cell treatment with the NF-κB pathway inhibitor, JSH-23, attenuated the activation of NF-κB pathway and the tumor promoting effects of cells induced by CMSS1 overexpression (Figure 6C–H). These results suggested that CMSS1 could promote HCC proliferation and migration via regulating the TNF/NF-κB signaling pathway.

Discussion

To further uncover the molecular mechanisms underlying the occurrence and development of HCC, bioinformatics analysis was carried out. The analysis revealed a new molecule, CMSS1, which was significantly associated with the proliferation of HCC cells. Functional studies demonstrated that CMSS1 could promote the proliferation and migration of HCC cells both in vitro and in vivo. The results further indicated that CMSS1 could activate the downstream TNF/NF-κB pathway, which exerted tumor-promoting effects. The above results highlighted the biological function and mechanism of CMSS1 in the progression of HCC, thus enhancing our understanding of the role of CMSS1 in the pathogenesis of HCC and providing novel promising biomarkers and treatment targets for HCC.

Normal cells divide and multiply in a stringently regulated manner. When this regulation is disrupted, cancer forms.[20] Therefore, almost all tumor cells have one common feature which is associated with cell proliferation, the activation of proliferation-related genes and repression of genes associated with proliferation inhibition, thereby allowing the tumor to grow without restriction.[21] In addition, it has been reported that cancer cell migration within tissues is a key process in the development of cancer.[22] Therefore, when cancer progresses and metastasizes, cells can move independently or collectively and spread to other organs, thus further promoting cancer development.[23] EMT serves a key role in the invasion and metastasis of cancer cells.[15,16] During EMT, epithelial cells lose their polarity,while E-cadherin is down-regulated, thus resulting in reduced cellular adhesion, which in turn makes it easier for cells to invade and migrate. At the same time, these cells acquire a mesenchymal phenotype, which is characterized by the enhanced expression of proteins, such as that of vimentin and N-cadherin.[24] Herein, CMSS1 overexpression significantly promoted the proliferation, migration and EMT process of HCC cells, thus highlighting its significant role in the development of HCC.

TNF is a significant cytokine, which primarily functions through two receptors, namely TNF receptor 1 (TNFR1) and TNFR2.[25] The combination of TNF and TNFR1 can lead to the activation of several signaling pathways, including the NF-κB, MAPK and Jun N-terminal kinase signaling pathways, which are involved in several biological processes, such as cell proliferation, migration and apoptosis, and inflammatory reactions.[26] A previous study indicated that the activation of the TNF signaling pathway was closely associated with the occurrence and development of numerous diseases, including but not limited to cancer, infectious diseases and autoimmune diseases.[27] The current study demonstrated that CMSS1 promoted the proliferation and migration of HCC cells through the activation of the TNF/NF-κB pathway. However, how CMSS1 could regulate the TNF/NF-κB pathway was not investigated, which is one of the limitations of the present study. Therefore, future research should integrate the functions of CMSS1 to address this gap.

Although there are few reports on CMSS1, it is currently considered as an RBP. RBPs are a class of highly conserved proteins that play a crucial role in the post-transcriptional regulation of gene expression. Increasing evidence has indicated that RBPs act via recognizing and binding to sequences on target transcripts through their RNA binding domains.[28] RBPs are also referred to as "clothes for the mRNA", ensuring that different mRNA regions, namely the 5′ and 3′ untranslated regions (UTRs) and the coding region, are sometimes covered or exposed, thus facilitating the translation process and the overall function of the protein.[29] Regarding the TNF pathway, it has been reported that there are five types of RBPs that can directly bind to the TNFα mRNA, namely TIA-1-related protein, T cell intracellular antigen-1, human antigen R, fragile-X-related protein 1 and tristetraprolin.[30] As with several other cellular factors, the 3′-UTR of the TNFα mRNA encompasses an AU-rich element (ARE), as well as a constitutive decay element.[31] A previous

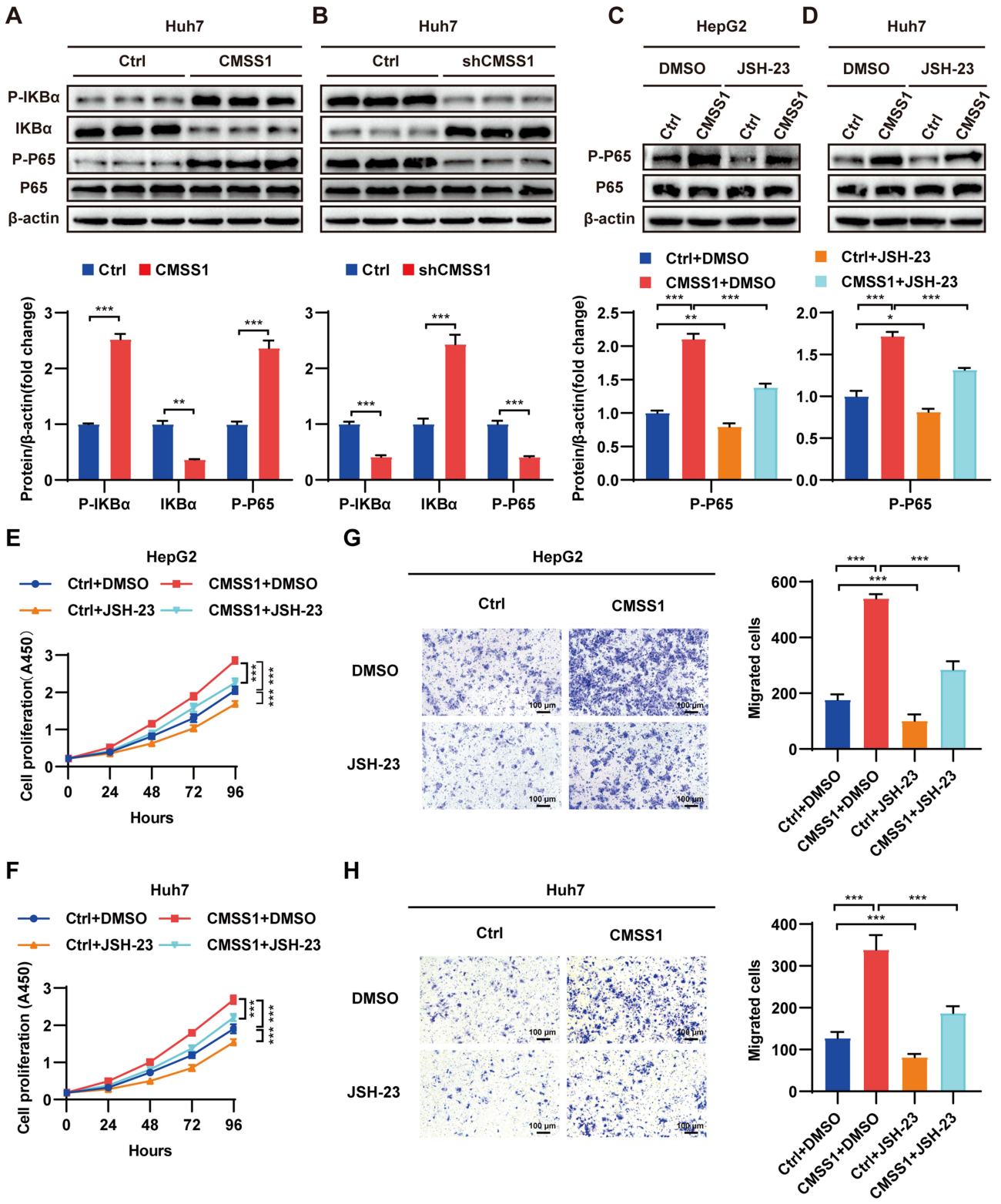

Figure 6 CMSS1 regulates the TNF/NF-κB signaling pathway. (**A**) Western blot assay showed the protein expression of NF-κB signaling pathway of Huh7 cells with control and CMSS1 overexpression groups. (**B**) Western blot assay showed the protein expression of NF-κB signaling pathway of Huh7 cells with control and CMSS1 knockdown groups. (**C** and **D**) Western blot assay showed that JSH-23 (1 μM) reversed the up-regulation of protein expression levels of NF-κB signaling pathway in HepG2 and Huh7 cells. (**E** and **F**) CCK-8 assay showed that JSH-23 (1 μM) reversed the enhanced proliferation capacity caused by CMSS1 overexpression in HepG2 and Huh7 cells. (**G** and **H**) Transwell migration assay showed that JSH-23 (1 μM) reversed the enhanced migration capacity caused by CMSS1 overexpression in HepG2 and Huh7 cells. All data are presented as the means ± SD, *p < 0.05; **p < 0.01; ***p < 0.001.

Abbreviation: ns, not significant.

https://doi.org/10.2147/JHC.S549003

study showed that ARE was negatively associated with mRNA stability, which could be mediated by RBPs.[32] Therefore, it was hypothesized that CMSS1 could affect the expression levels of TNFα via combining with its ARE structure, thus affecting its mRNA stability. Future studies, such as RNA immunoprecipitation (RIP) assays, were necessary to experimentally validate this interaction and its functional role in the TNF pathway.

In summary, the current study revealed the biological function of CMSS1 in the development of HCC. The results demonstrated that CMSS1 could regulate the proliferation and migration of HCC cells via modulating the TNF/NF-κB signaling pathway. Overall, the above findings suggested that CMSS1 could be a potential therapeutic target of HCC. Future studies focusing on the detailed molecular mechanisms and the development of targeted strategies against CMSS1 are warranted to translate these findings into clinical applications.

Limitations of the Study

Although we inferred the potential mechanism by which CMSS1 regulated the TNF pathway in the discussion, further experimental verification is still required.

Ethics Approval and Consent to Participate

All animal experimental protocols were approved by the Animal Care and Use Committee of the Renmin Hospital of Wuhan University and performed in accordance with the "Laboratory animal—Guideline for welfare and ethics" (GB/T 35892-2018) issued by the Standardization Administration of China.

Funding

This work was supported by grants from the National Natural Science Foundation of China (81970011 [to P. Z.]) and the Basic Medicine-Clinical Medicine Transformation Collaborative Fund of Zhongnan Hospital of Wuhan University (grant no.: ZNLH202211 [to P. Z.]).

Disclosure

The authors report no conflicts of interest in this work.

References

1. Bray F, Laversanne M, Sung H, et al. Global cancer statistics 2022: GLOBOCAN estimates of incidence and mortality worldwide for 36 cancers in 185 countries. *CA Cancer J Clin*. 2024;74(3):229–263. doi:10.3322/caac.21834
2. Ladd AD, Duarte S, Sahin I, Zarrinpar A. Mechanisms of drug resistance in HCC. *Hepatology*. 2024;79(4):926–940. doi:10.1097/HEP.0000000000000237
3. Toh MR, Wong EYT, Wong SH, et al. Global epidemiology and genetics of hepatocellular carcinoma. *Gastroenterology*. 2023;164(5):766–782. doi:10.1053/j.gastro.2023.01.033
4. Singal AG, Kanwal F, Llovet JM. Global trends in hepatocellular carcinoma epidemiology: implications for screening, prevention and therapy. *Nat Rev Clin Oncol*. 2023;20(12):864–884. doi:10.1038/s41571-023-00825-3
5. Yang C, Zhang H, Zhang L, et al. Evolving therapeutic landscape of advanced hepatocellular carcinoma. *Nat Rev Gastroenterol Hepatol*. 2023;20(4):203–222. doi:10.1038/s41575-022-00704-9
6. Yang X, Yang C, Zhang S, et al. Precision treatment in advanced hepatocellular carcinoma. *Cancer Cell*. 2024;42(2):180–197. doi:10.1016/j.ccell.2024.01.007
7. Zucman-Rossi J, Villanueva A, Nault JC, Llovet JM. Genetic landscape and biomarkers of hepatocellular carcinoma. *Gastroenterology*. 2015;149(5):1226–1239.e4. doi:10.1053/j.gastro.2015.05.061
8. Rebouissou S, Nault JC. Advances in molecular classification and precision oncology in hepatocellular carcinoma. *J Hepatol*. 2020;72(2):215–229. doi:10.1016/j.jhep.2019.08.017
9. Llovet JM, Kelley RK, Villanueva A, et al. Hepatocellular carcinoma. *Nat Rev Dis Primers*. 2021;7(1):6. doi:10.1038/s41572-020-00240-3
10. Villanueva A. Hepatocellular Carcinoma. *N Engl J Med*. 2019;380(15):1450–1462. doi:10.1056/NEJMra1713263
11. Xie Y, Luo X, He H, Pan T, He Y. Identification of an individualized RNA binding protein-based prognostic signature for diffuse large B-cell lymphoma. *Cancer Med*. 2021;10(8):2703–2713. doi:10.1002/cam4.3859
12. Gu W, Li H, Sun L, et al. The RNA-binding protein CMSS1 promotes the progression of non-small cell lung cancer by regulating the telomerase protein subunit hTERT. *Life Sci*. 2025;361:123321. doi:10.1016/j.lfs.2024.123321
13. Fan Z, Liu W, Gao Z, Liu Y, Hai H, Lv Z. CMSS1: a RNA binding protein with pivotal roles in non-small cell lung cancer progression and prognosis. *BMC Cancer*. 2025;25(1):688. doi:10.1186/s12885-025-14044-9
14. Wei S, Tan J, Huang X, et al. Metastasis and basement membrane-related signature enhances hepatocellular carcinoma prognosis and diagnosis by integrating single-cell RNA sequencing analysis and immune microenvironment assessment. *J Transl Med*. 2024;22(1):711. doi:10.1186/s12967-024-05493-0

15. Huang Y, Hong W, Wei X. The molecular mechanisms and therapeutic strategies of EMT in tumor progression and metastasis. *J Hematol Oncol*. 2022;15(1):129. doi:10.1186/s13045-022-01347-8
16. Mittal V. Epithelial mesenchymal transition in tumor metastasis. *Annu Rev Pathol*. 2018;13(1):395–412. doi:10.1146/annurev-pathol-020117-043854
17. Chen L, Zhou J, Li L, et al. SLC39A7 promotes malignant behaviors in glioma via the TNF-α-mediated NF-κB signaling pathway. *J Cancer*. 2021;12(15):4530–4541. doi:10.7150/jca.54158
18. Han MT, Pei H, Sun QQ, et al. ZY-444 inhibits the growth and metastasis of prostate cancer by targeting TNFAIP3 through TNF signaling pathway. *Am J Cancer Res*. 2023;13(4):1533–1546.
19. Liu W, Wang H, Jian C, et al. The RNF26/CBX7 axis modulates the TNF pathway to promote cell proliferation and regulate sensitivity to TKIs in ccRCC. *Int J Biol Sci*. 2022;18(5):2132–2145. doi:10.7150/ijbs.69325
20. Liu J, Peng Y, Wei W. Cell cycle on the crossroad of tumorigenesis and cancer therapy. *Trends Cell Biol*. 2022;32(1):30–44. doi:10.1016/j.tcb.2021.07.001
21. Long ZJ, Wang JD, Xu JQ, Lei XX, Liu Q. cGAS/STING cross-talks with cell cycle and potentiates cancer immunotherapy. *Mol Ther*. 2022;30(3):1006–1017. doi:10.1016/j.ymthe.2022.01.044
22. Campbell K, Casanova J. A common framework for EMT and collective cell migration. *Development*. 2016;143(23):4291–4300. doi:10.1242/dev.139071
23. Elisha Y, Kalchenko V, Kuznetsov Y, Geiger B. Dual role of E-cadherin in the regulation of invasive collective migration of mammary carcinoma cells. *Sci Rep*. 2018;8(1):4986. doi:10.1038/s41598-018-22940-3
24. Xu Q, Liu X, Liu Z, et al. MicroRNA-1296 inhibits metastasis and epithelial-mesenchymal transition of hepatocellular carcinoma by targeting SRPK1-mediated PI3K/AKT pathway. *Mol Cancer*. 2017;16(1):103. doi:10.1186/s12943-017-0675-y
25. Croft M, Siegel RM. Beyond TNF: TNF superfamily cytokines as targets for the treatment of rheumatic diseases. *Nat Rev Rheumatol*. 2017;13(4):217–233. doi:10.1038/nrrheum.2017.22
26. van Loo G, Bertrand MJM. Death by TNF: a road to inflammation. *Nat Rev Immunol*. 2023;23(5):289–303. doi:10.1038/s41577-022-00792-3
27. Siegmund D, Wajant H. TNF and TNF receptors as therapeutic targets for rheumatic diseases and beyond. *Nat Rev Rheumatol*. 2023;19(9):576–591. doi:10.1038/s41584-023-01002-7
28. Hentze MW, Castello A, Schwarzl T, Preiss T. A brave new world of RNA-binding proteins. *Nat Rev Mol Cell Biol*. 2018;19(5):327–341. doi:10.1038/nrm.2017.130
29. Singh G, Pratt G, Yeo GW, Moore MJ. The clothes make the mRNA: past and present trends in mRNP fashion. *Annu Rev Biochem*. 2015;84(1):325–354. doi:10.1146/annurev-biochem-080111-092106
30. Khera TK, Dick AD, Nicholson LB. Mechanisms of TNFα regulation in uveitis: focus on RNA-binding proteins. *Prog Retin Eye Res*. 2010;29(6):610–621. doi:10.1016/j.preteyeres.2010.08.003
31. Codutti L, Leppek K, Zálešák J, et al. A distinct, sequence-induced conformation is required for recognition of the constitutive decay element RNA by roquin. *Structure*. 2015;23(8):1437–1447. doi:10.1016/j.str.2015.06.001
32. Zhang Z, Guo M, Li Y, et al. RNA-binding protein ZFP36/TTP protects against ferroptosis by regulating autophagy signaling pathway in hepatic stellate cells. *Autophagy*. 2020;16(8):1482–1505. doi:10.1080/15548627.2019.1687985